J Electroceram (2012) 28:20–26
DOI 10.1007/s10832-011-9673-4

Electro-caloric behaviors of lead-free $Bi_{0.5}Na_{0.5}TiO_3$-$BaTiO_3$ ceramics

Xiu-Cheng Zheng · Guang-Ping Zheng · Zheng Lin · Zhi-Yuan Jiang

Received: 4 August 2011 / Accepted: 24 November 2011 / Published online: 7 December 2011

Abstract Electro-caloric (EC) properties of lead-free $Ba_{0.5}Na_{0.5}TiO_3$-$xBaTiO_3$ (BNT-xBT) ceramics prepared by citrate method are investigated at temperatures of 30–250°C. Based on thermodynamics calculations, BNT-xBT (x=0, 0.05, 0.06, 0.1, 0.25, 0.3) are found to show EC effects different with other lead-based or lead-free ferroelectric ceramics, i.e., they absorb heats (refrigeration effect) during the processes of field application while other ferroelectric ceramics show refrigeration effect during the processes of field removal. The EC temperature change of BNT-xBT can be as large as 2.1°C under an electric field of 60 kV/cm, which is larger than most of the lead-free ferroelectric bulk ceramics. When x is close to the morphotropic phase boundary (x~0.06–0.1), the EC temperature change of BNT-xBT shows a maximum near the ferroelectric to anti-ferroelectric transition temperature, which is characterized by dynamic mechanical analysis. This study suggests that these lead-free ferroelectric materials are promising in the practical application as EC coolers.

Keywords Ferroelectrics · Electro-caloric effect · Structural phase transformations

1 Introduction

Electro-caloric (EC) effect in ferroelectric materials is of great interest in the past decade because of the increasing demand on cooling solution for micro- and nano-electronic devices which have high-power and high-density heat-generating components. Unlike other solid-state refrigeration technologies, ferroelectric cooler based on the principle of EC effect could be small and energy efficient [1]. In all of the ferroelectric (FE) materials found to date, lead-based ferroelectric materials such as lead zirconate titanate (PZT) [2], and lead magnesium niobate-lead titanate (PMN-PT) [3] have been extensively investigated in terms of their EC effects. Although lead-based ferroelectrics show excellent EC behaviors, for example, the EC refrigeration temperature change can be as large as 12°C in PZT thin films [4], it is desirable that environmentally friendly lead-free ferroelectrics can be used for EC coolers in microelectronic devices.

Recently, several groups of lead-free ferroelectric ceramics exhibiting excellent EC effect have been explored [5, 6]. Barium titanate (BT) thick-film multilayered structures [7] are found to show the EC refrigeration temperature change of 4°C, which is slightly less than that of lead-based thin films [4]. To further search for lead-free ferroelectric ceramics whose EC refrigeration properties are comparable with those of lead-based ones, it is important in investigating the EC behaviors of other lead-free materials exhibiting better ferroelectric properties than those of barium titanate.

Bismuth sodium titanate ($Bi_{0.5}Na_{0.5}TiO_3$, abbreviated as BNT) is one of the most important lead-free materials with excellent ferroelectric properties such as large remanent polarization (Pr ~38 μC/cm^2) and large coercive field (Ec ~73 kV/cm) [8]. These properties make BNT very promising as excellent EC material since the EC temperature change usually increases with increasing remanent polarization of the material and the applied electric field. However, there are two disadvantages of BNT if it is developed as EC materials for cooling microelectronic devices. First, BNT has a ferroelectric to anti-ferroelectric (AFE) transition around 150°C and an AFE to paraelectric (PE) transition around 320°C [9]. The EC temperature change usually shows a

X.-C. Zheng · G.-P. Zheng (✉) · Z. Lin · Z.-Y. Jiang
Department of Mechanical Engineering, The Hong Kong Polytechnic University,
Kowloon, Hong Kong
e-mail: mmzheng@polyu.edu.hk

maximum around the critical temperatures of these transitions while in a practical EC cooler for microelectronic devices the operating temperature is between ambient and 85°C. Thus BNT may not be efficient if it is operated as EC coolers. Second, BNT has relatively large leakage current because of the loss of bismuth content during conventional solid state reaction processing, which will deteriorate its EC refrigeration effect under large electric fields.

In this study, we investigate the EC behaviors of BNT-xBT ceramics prepared with citrate method, which could solve the above-mentioned issues when appropriate BT content x of this ceramics is chosen. This is because the structural and ferroelectric properties of BNT-xBT significantly depend on x and their leakage currents could be much smaller than that of BNT when x and the processing procedure are carefully optimized. It is the first systematic study on the EC effects in these ceramics.

2 Preparation and characterization of the BNT-xBT ceramics

BNT-xBT samples were prepared by citrate method. Reagent grade $NaNO_3$, $Ba(NO_3)_2$, $Bi(NO_3)_3{\cdot}5H_2O$, citric acid and tetrabutyl titanate were used as starting materials to prepare BNT-xBT powders with the nominal composition of $(Bi_{0.5}Na_{0.5})_{1-x}Ba_xTiO_3$ (x=0, 0.05, 0.06, 0.1, 0.25, 0.3). The mole ratio of citric acid to total metal cation content was 1.60. The precursor solution was dehydrated in an oven at 105°C to form a sol. Subsequent heating at a higher temperature of 160°C yielded a black gel. The gel was pulverized and then calcined at 280°C for 1 h and 600°C for 2 h in air to form the powders. Figure 1(a) shows the X-ray diffraction (XRD) of these powders using a Philips PW3040/60 diffractometer at room temperature with nickel filtered Cu Kα radiation (λ=1.5418 Å).

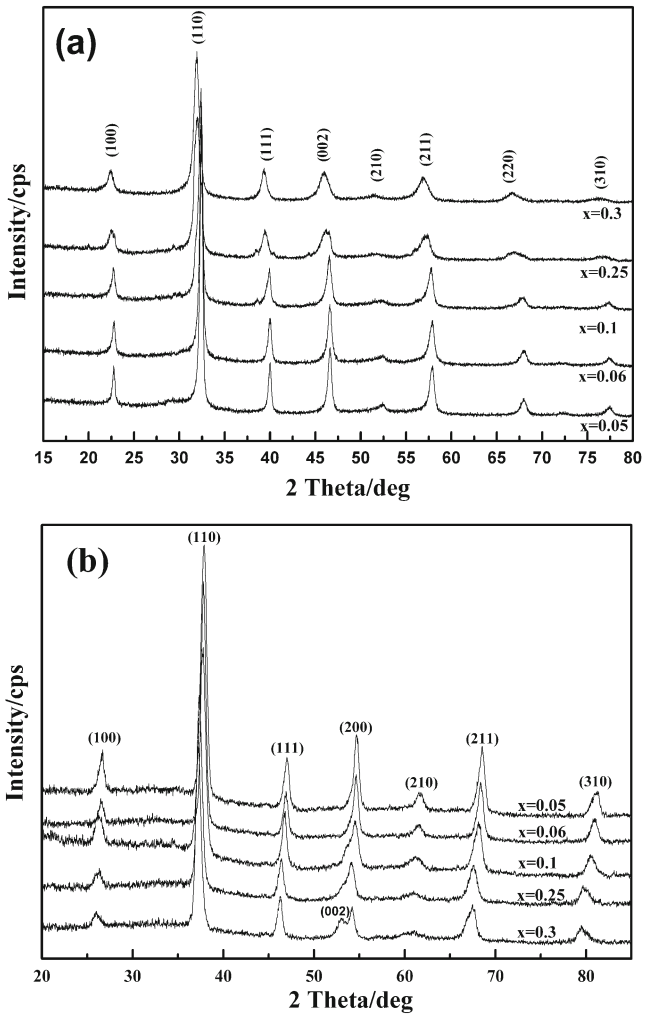

Fig. 1 (**a**) XRD (Cu Kα radiation, λ=1.5418 Å) patterns of the BNT-xBT powders. (**b**) XRD (Co Kα radiation, λ=1.79021 Å) patterns of the BNT-xBT ceramics. The (002)/(200) peak splitting in the 2θ range of 51–57° is indicated

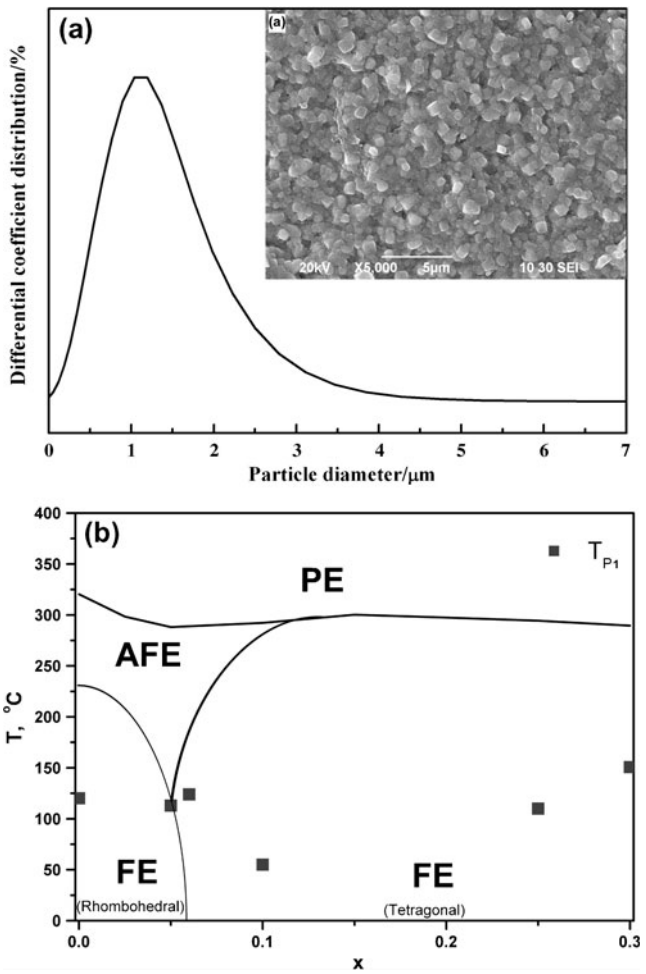

Fig. 2 (**a**) Particle size analysis results and SEM image (inset) of BNT-0.06BT samples. (**b**) Phase diagram of BNT-xBT. The solid curves are schematic of phase boundaries given in Ref. [9]. The symbols are the structural transformation temperatures T_{p1} determined from DMA

The prepared BNT-xBT powders were uniaxially pressed at 10 tons in the form of discs with a diameter of 10 mm. The green discs were heated at 600°C for 6 h to remove the binder. The calcined discs were sintered at 1100°C in ambient atmosphere for 2 h to form the ceramics. Figure 1(b) shows the XRD patterns of BNT-xBT ceramics using a Bruker D8 advance diffractometer with Co Kα radiation (λ=1.79021 Å). Figure 1 indicates that the BNT-xBT powders and ceramics are homogeneous solid solutions with a pure perovskite phase.

From the XRD patterns of the as-prepared BNT-xBT powders and the ceramics in the 2θ range of 44–49° detected with Cu Kα radiation and 51–57° detected with Co Kα radiation, as shown in Fig. 1(a) and (b) respectively, it can be seen that the strength of (200) peak reduces with increasing BT content x, while the strength of (002) peak increases with the increase of BT content, especially in the BNT-xBT with x>0.1. Because the (002)/(200) peak splitting usually indicates the exiting of perovskite phase with a tetragonal symmetry [10], the crystal structure of BNT-xBT at room temperature could be identified as rhombohedral and tetragonal structures when x≤0.1 and x>0.1, respectively.

Figure 2(a) shows the typical particle size distribution of a BNT-xBT sample measured by a Rise-2006 laser particle size analyzer. The SEM image of the BNT-xBT ceramics sample also indicates that they have dense, fine-grained microstructures, as shown in the inset of Fig. 2(a) for BNT-0.06BT.

The BNT-xBT ceramics have rich structural phase transformations accompanying by the transitions of their ferroelectric properties. As shown in the schematic of phase diagram [9] in Fig. 2(b), there is a morphotropic phase boundary (MPB) around x=0.06 distinguishing the rhombohedral and tetragonal structures which are all in FE states at room temperature. At elevated temperature the

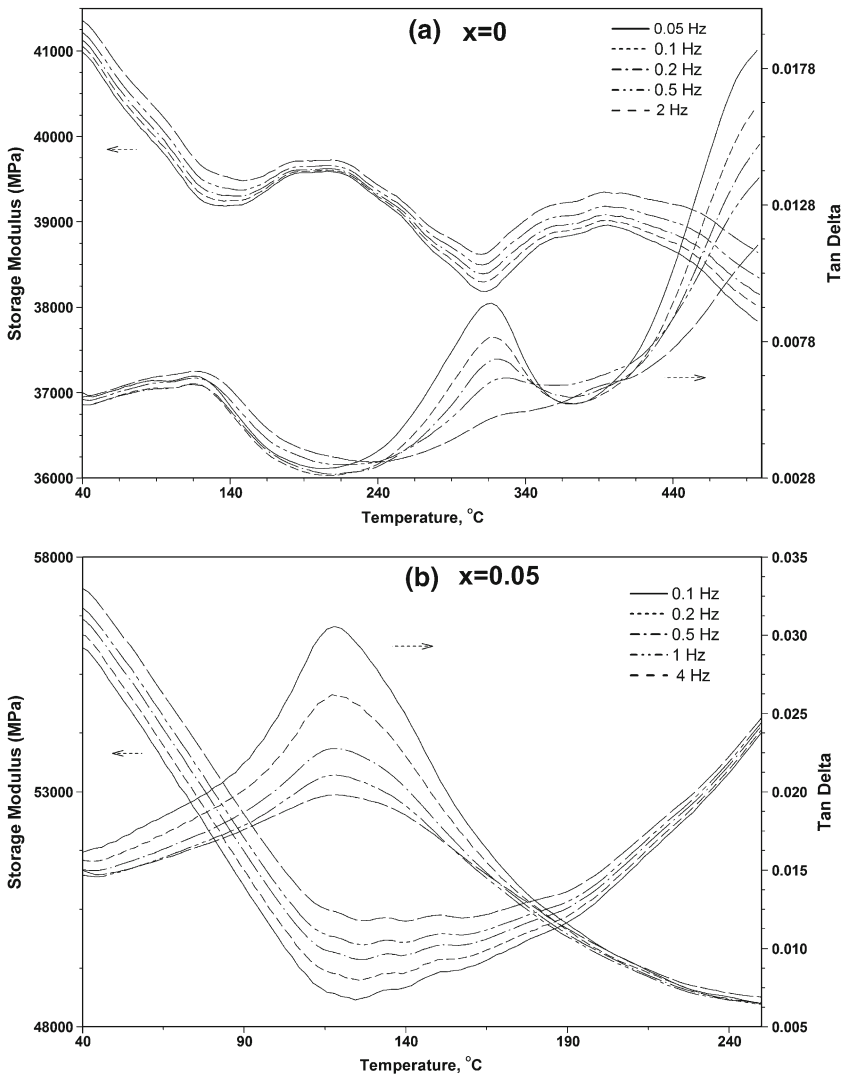

Fig. 3 Storage modulus and mechanical loss (tanδ) values of BNT-xBT under different frequencies. (**a**) BNT ceramic. (**b**) BNT-0.05BT ceramic

ceramics change from an FE state into an AFE state before they become paraelectric at higher temperatures. The phase transformations in BNT-xBT could be well characterized by the dynamic mechanical analysis (DMA) as shown in Fig. 3. In BNT ceramics, from room temperature to 500°C, the first peak of the mechanical loss (*tanδ*) indicates that there is an FE-to-AFE transition at T_{p1}=130°C; the second peak at T_{p2}= 320°C corresponds to the AFE-to-PE transition. Both *tanδ* peaks are associated with significant lattice softening as indicated by the cusps of the storage modulus, suggesting that those ferroelectric changes are caused by the structural transformations. Using DMA, the FE-to-AFE and AFE-to-PE transition temperatures can be well determined. Since we are interested in the EC effect of BNT-xBT around 100°C, we emphasize our analysis on the structural transformation corresponding to the FE-to-AFE transition using DMA. Figure 3(b) shows typical DMA results at temperatures around T_{p1}. It can be found that

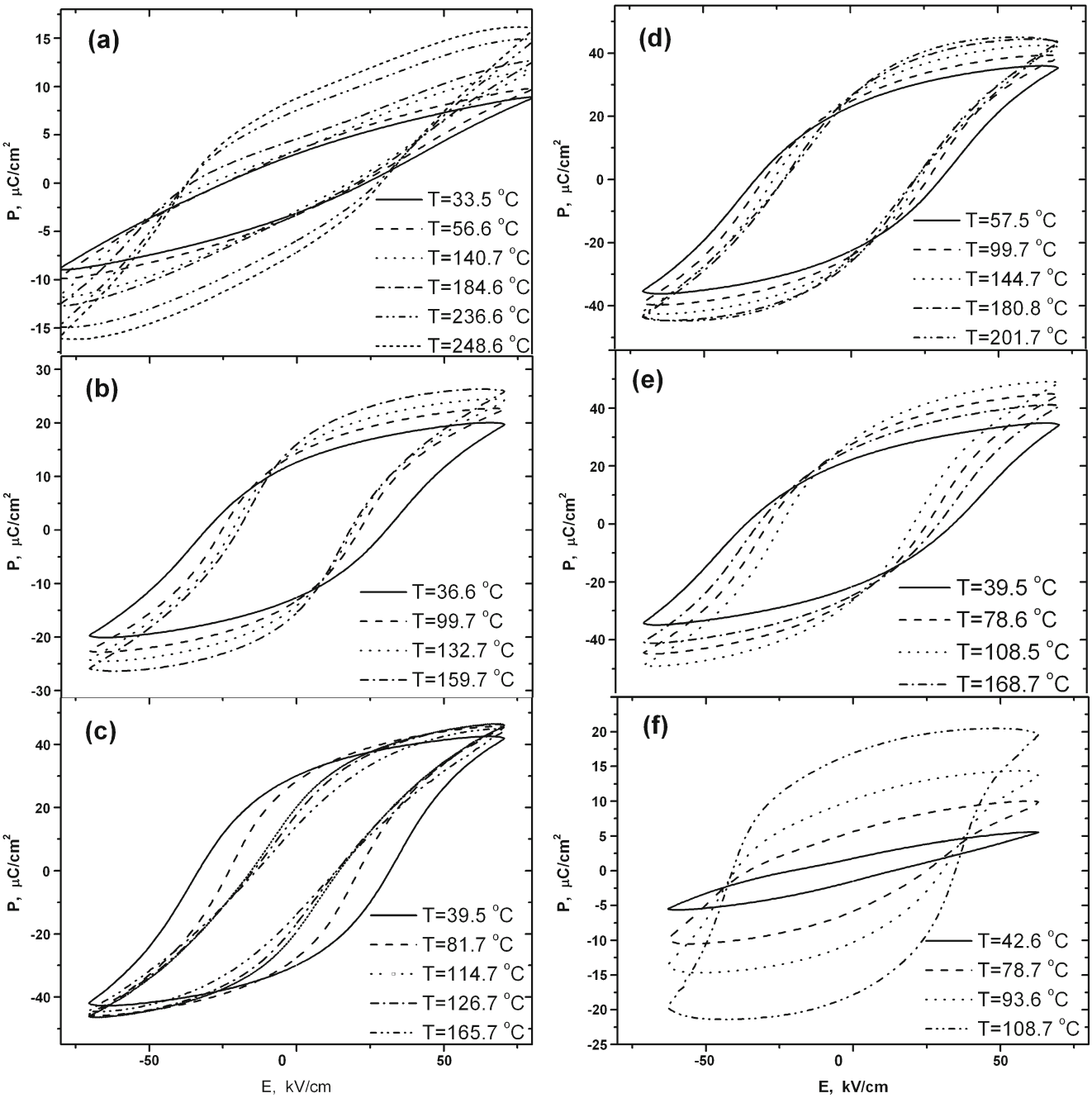

Fig. 4 P-E hysteresis loops of BNT-xBT ceramics at different temperatures. (**a**) x=0. (**b**) x=0.05. (**c**) x=0.06. (**d**) x=0.1. (**e**) x=0.25. (**f**) x=0.3

the height of *tanδ* peak increases with decreasing frequency. T_{p1} is independent of frequency and the elastic modulus shows a cusp at a temperature 2–10°C higher than T_{p1}. All these characteristics of DMA results suggest that the FE-to-AFE transition could be caused by the incommensurate modulation [11] of rhombohedral structures.

The relation between T_{p1} and x is shown in Fig. 2(b). Significant drop of T_{p1} is seen at x=0.1, close to the MPB. For x=0, 0.05, 0.06, 0.1, 0.25, 0.3, T_{p1} are all below 150°C.

3 EC behaviors of the BNT-xBT ceramics

The EC behaviors of BNT-xBT are characterized by the temperature change ΔT calculated by thermodynamics Maxwell's relations:

$$\Delta T = -\frac{1}{\rho C}\int_{E_1}^{E_2} T\left(\frac{\partial P}{\partial T}\right)_E dE, \quad (1)$$

where $\boldsymbol{\rho}$ is the density, C is heat capacity and $(\partial \boldsymbol{P}/\partial \boldsymbol{T})_E$ is the pyroelectric coefficient of ferroelectric material under a

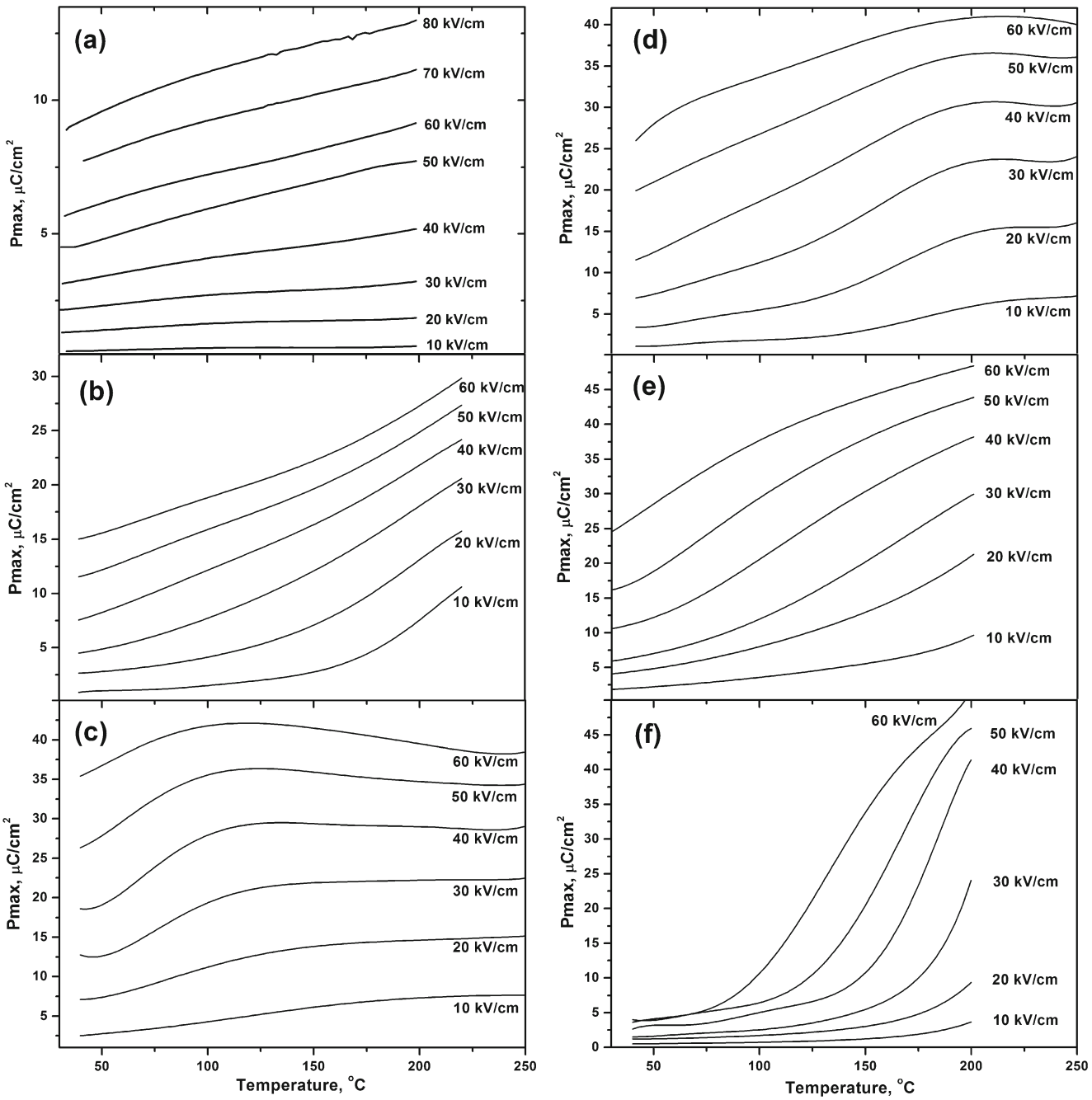

Fig. 5 Polarization of BNT-xBT ceramics under applied electric fields of 10, 20, 30, 40, 50, 60 kV/cm at different temperatures. (**a**) x=0; (**b**) x=0.05; (**c**) x=0.06; (**d**) x=0.1; (**e**) x=0.25; (**f**) x=0.3

certain electric field ***E*** varying from E_1 to E_2. The polarization ***P*** of the sample is determined from the ferroelectric hysteresis loops (P-E loops) using a ferroelectric test system (TF Analyzer 2000E, aixACCT).

Figure 4 shows the P-E loops of BNT-xBT ceramic samples at various temperatures. The effects of applied electric field on the temperature-dependent polarizations measured from the P-E loops are shown in Fig. 5. Under the applied electric fields of 10–60 kV/cm, the leakage currents of all the samples are found to be lower than 20 μA except for BNT-0.3BT at temperatures higher than 150°C. At room temperature BNT-0.06 BT is found to possess the best ferroelectric properties, e.g., the largest remanent polarization among all samples.

The refrigeration temperature change ΔT is calculated by Eq. 1 with E_1=10 kV/cm and E_2=60 kV/cm. Figure 6 shows ΔT of BNT-xBT at different temperatures. Remarkably, ΔT is found to be negative which is opposite to EC behaviors of other ferroelectric materials. The negative ΔT suggests that BNT-xBT absorb heats (refrigeration effect) during the processes of field applications while other ferroelectric ceramics show refrigeration effect during the processes of field removal. The EC behaviors of different BNT-xBT ceramics can be compared in Fig. 6. BNT shows very small refrigeration temperature change $|\Delta T|$<0.15°C, which is in the same magnitude as that of BT ceramics [2]. While BNT-xBT ceramics exhibit much larger refrigeration temperature changes. $|\Delta T|$ can be as large as 2.1°C in BNT-0.3BT at 150°C which is larger than most of the lead-based [2] and lead-free [2] ferroelectric bulk ceramics. When the BT content (x=0.06, or 0.1) is close to the MPB, $|\Delta T|$ shows a maximum around 50–70°C, close to the FE-to-AFE transition temperatures T_{p1} of the samples. Although $|\Delta T|$ of BNT-0.06BT and BNT-0.1BT around T=50–70°C are not the largest among all BNT-xBT samples, these two ceramics are promising EC materials to be developed as EC coolers for microelectronic devices. Not only because their leakage currents (<10 μA) are smaller than those of other samples, but also because they show the maximum $|\Delta T|$ between 50–70°C, the service temperatures at which most of the microelectronic devices will be cooled down. The fact that BNT-0.06BT shows the best EC behaviors could result from its excellent ferroelectric properties and sample quality as shown in Figs. 4 and 2(a) respectively.

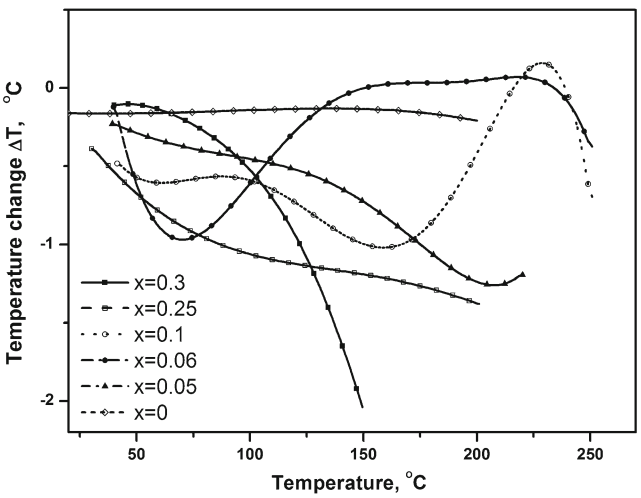

Fig. 6 EC refrigeration temperature change of BNT-xBT ceramics when the applied field is changed from 10 to 60 kV/cm

The anomaly in EC effect of BNT-xBT can be explained from Figs. 4 and 5 by using Eq. 1. Because of the FE-to-AFE transition processes at elevated temperatures, the polarizations of BNT-xBT increases with increasing temperature. Hence the positive pyroelectric coefficient leads to a negative ΔT. On one hand, the increases of polarizations of BNT-xBT ($x\neq0$) with increasing temperature can be explained by the incommensurate modulation of rhombohedral structures associated with the FE-to-AFE transition. BNT-xBT shows typical ferroelectric relaxor behaviors and the polarization of the rhombohedral BNT-xBT in the FE state could be smaller than that in the AFE state due to the ordering of the dipolar regions which is caused by the incommensurate modulation of rhombohedral structures. On the other hand, it should be noted that such abnormal EC refrigeration behaviors in BNT-xBT are predicted by the thermodynamics Maxwell's relation which may not well characterize the relation between the polarization and the entropy changes during the FE-to-AFE transition process. In the future research, direct measurement of the refrigeration effect or ΔT could be useful in clarifying the abnormal EC behaviors of BNT-xBT observed in this study.

4 Conclusions

In this study, we investigate the EC behaviors of lead-free BNT-xBT ceramics prepared with citrate method. The refrigeration effect of these ceramics is found to result from the application of an electric field, instead of the removal of applied fields in other EC materials. Such phenomenon is ascribed to the transition of an FE state to an AFE state at elevated temperature. The EC temperature change of BNT-xBT can be as large as 2.1°C under an electric field of 60 kV/cm, which is larger than most of the lead-free or lead-based ferroelectric bulk ceramics. When x is close to the morphotropic phase boundary (x~0.06–0.1), the EC temperature change of BNT-xBT shows a maximum around 50–70°C, which is close to the region of transition between a ferroelectric state and an anti-ferroelectric state. This study suggests that BNT-xBT is promising in the practical application of these lead-free ferroelectric materials as EC coolers.

Acknowledgements The authors are grateful for the financial supports provided by the Innovative Technology Funds of Hong Kong (Project No. ITS/314/09), the Research Funds of Hong Kong Polytechnic University (Project No. A-PK81).

References

1. R. Radebaugh, W.N. Lawless, J.D. Siegwarth, A.J. Morrow, Cryogenics **19**, 187–208 (1979)
2. P.D. Thacher, J Appl Phys **39**, 1996 (1968)
3. J. Perantie, J. Hagberg, A. Uusimaki, H. Jantunen, Appl Phys Lett **94**, 102903 (2009)
4. S. Mischenko, Q. Zhang, J.F. Scott, R.W. Whatmore, N.D. Mathur, Science **311**, 1270 (2006)
5. H. Chen, T.L. Tian, X.M. Wu, Y. Yang, L.T. Liu, Appl Phys Lett **94**, 182902 (2009)
6. Y. Bai, G.P. Zheng, S.Q. Shi, Appl Phys Lett **96**, 192902 (2010)
7. Y. Bai, G.P. Zheng, S.Q. Shi, J Appl Phys **108**, 104101 (2010)
8. T. Takenaka, T. Okuda, K. Takegahara, Ferroelectrics **196**, 175–178 (1997)
9. Y. Hiruma, Y. Watanabe, H. Nagata, T. Takenaka, Key Eng Mater **350**, 93 (2007)
10. M. Chen, Q. Xu, B.H. Kim, B.K. Ahn, J.H. Ko, W.J. Kang, O.J. Nam, J Eur Ceram Soc **28**, 843–849 (2008)
11. M. Barmatz, L.R. Testardi, F.J. di Salvo, Phys Rev B **12**, 4367–4376 (1975)